

Article

Mineralogical and Sedimentological Characterization of the Clay-Rich Sediments from Ases Cave (Cova Dets Ases, Mallorca, Spain): Origin and Classification

Ana Entrena ^{1,2,3,*}, Joan J. Fornós ^{2,3} , Luis F. Auqué ¹, Francesc Gràcia ^{2,3} and Elisa Laita ⁴ 

¹ Department of Earth Sciences, Faculty of Sciences, University of Zaragoza, Pedro Cerbuna 12, 50009 Zaragoza, Spain

² Earth Sciences Research Group, University of the Balearic Islands, Crta. Valldemossa, Km 7.5, 07122 Palma, Spain

³ Societat Espeleològica Balear (SEB), Margarida Xirgu, 16, 07011 Palma, Spain

⁴ IUCA-Department of Earth Sciences, Faculty of Sciences, University of Zaragoza, Pedro Cerbuna 12, 50009 Zaragoza, Spain

* Correspondence: a.entrena.f@gmail.com

Abstract: The Mallorca coastal caves present large amounts of speleothems that have been studied for decades. However, the sedimentary deposits also present in these cases have not been given the same attention. This work is the first study entirely focused on these deposits, specifically the ones found in the Ases cave. These deposits are formed by clay minerals (illitic phases, kaolinite, smectite, and chlorite), calcite and quartz, and minor proportions of dolomite, albite, orthoclase, hematite, and goethite. The grain size and the electron microscopy studies suggested the presence of different sedimentation processes (bedrock degradation, creep or saltation, and suspension) and different origins (authigenic and detrital origins) for the different sediments. Based on these differences, two types of deposits were characterized: autochthonous and allochthonous deposits. The first ones are located on the floor of chambers and corridors in subaqueous zones, indicating the stability of the mixing zone (and therefore the sea level) over time. The second ones appear filling voids on the walls and the ceiling in the terrestrial zone, evidencing the filling of the cavity in the presence of water (during a wet period). These results are very important to complete the understanding of the caves and their evolution and support the relevance of these materials in paleoenvironmental studies.

Keywords: caves; autochthonous sediments; allochthonous sediments; kaolinite; smectite; weathering



Citation: Entrena, A.; Fornós, J.J.; Auqué, L.F.; Gràcia, F.; Laita, E. Mineralogical and Sedimentological Characterization of the Clay-Rich Sediments from Ases Cave (Cova Dets Ases, Mallorca, Spain): Origin and Classification. *Minerals* **2022**, *12*, 1473. <https://doi.org/10.3390/min12111473>

Academic Editor: Ricardo Ferreira Louro Silva

Received: 10 October 2022

Accepted: 19 November 2022

Published: 21 November 2022

Publisher's Note: MDPI stays neutral with regard to jurisdictional claims in published maps and institutional affiliations.



Copyright: © 2022 by the authors. Licensee MDPI, Basel, Switzerland. This article is an open access article distributed under the terms and conditions of the Creative Commons Attribution (CC BY) license (<https://creativecommons.org/licenses/by/4.0/>).

1. Introduction

Caves are considered sites of great interest to extract paleoclimatic information, but relevant studies have mainly focused on speleothem deposits (e.g., stalactites and stalagmites), leaving the sedimentary deposits outside [1–3] among others. The study of cave sediments from a mineralogical and sedimentological point of view can provide information of interest about their origin and the paleoenvironmental conditions at the local scale [4–6].

The first classification of cave sediments was proposed by Ford and Williams [7], who distinguished between autochthonous and allochthonous deposits. Autochthonous sediments can be associated with different origins [5,8–11]: (1) the dissolution of the bedrock during the speleogenesis; (2) diagenetic processes related to the presence of sulfuric groundwaters; and (3) the formation of minerals by microbiological alteration of the bedrock or other minerals.

However, most of the cavities worldwide have allochthonous sediments related to the erosion, transport, and subsequent sedimentation processes, and they are commonly composed by soil materials from the exterior of the caves. These sediments can provide

information about the soil composition and/or about the climatic variations that take place during erosion and deposition processes [5,12,13]. These deposits are associated (1) with flow movements of fluvial courses that circulate or circulated inside the cavity [14]; (2) with flooding of river courses, or (3) with episodic storm events [4,5,11,15]. Although less common, there are also aeolian deposits, such as those found in Jenolan cave, New South Wales [9], or the aeolianites deposits associated with the entrance in Mallorca littoral caves [16], deposits related with volcanoclastic or glacial origins [9], and precipitates associated with thermal or hydrothermal processes [17]. A special mention should be made of the sedimentary deposits located in caves and sinkholes in Bermudas related directly to the variations of the sea level allowing their reconstruction [6].

The data needed to characterize the deposits in a cave are their location in the cavity and their mineralogical and crystal morphological information obtained by means of techniques, such as X-ray diffraction or electron microscopy [8]. The typical mineral assemblages found in sedimentary deposits inside caves are constituted by calcite, dolomite, and/or aragonite (from the weathering processes of the bedrock or the speleothem), as well as by quartz, feldspar, and clay minerals (from impurities or from allochthonous sources) [5,8,11,18]. The case of clay minerals is slightly more complex because they can have both, detrital, and authigenic origins. Their detrital origin is related to soils or sediments transported into the cave. The authigenic formation occurs through the weathering of previous phases present in the sediments [4,19,20]. Moreover, clay minerals can also be inherited from the weathering of the bedrock. The most common clay minerals reported in caves worldwide are illite and kaolinite [9,13,15]. Occasionally, montmorillonite and other phyllosilicates such as muscovite have also been described [4,8,17].

The speleogenetic development and the present conditions of the Mallorca Island are the result of the environmental evolution of the area and its proximity to the coast [21]. These two factors have generated the worldwide known Drac cave (touristic cave) and the Cova des Pas de Vallgornera (the largest cave in Europe, located in the same materials but in the south part of the island), as well as others equally interesting although not so well known, such as the Ases cave (Cova dels Ases), where this work has been developed.

Like the rest of the caves located in the eastern side of the Mallorca Island, the Ases cave was formed by dissolution processes in favor of the preferential routes represented by the reef systems present in the carved rock. It has 825 m of terrestrial length and 1000 m of subaqueous length. The karst evolution is produced by the collapse of large blocks that gives rise to large underground rooms connected by narrow passages [22]. In the last tens of thousands of years and until the present day, various types of speleothems (stalactites, stalagmites, rafts, gourds, phreatic overgrowths, etc.) have grown and some sedimentary materials have been deposited in the chambers and galleries.

So far, the few field works carried out on the sedimentary deposits inside the coastal carbonate karst systems in Mallorca indicate that most of this material is related to granular disaggregation and bedrock collapse and fall events that must have happened due to destabilizations and readjustments associated to the cave formation and to the seawater level fluctuations [16,23–28]. On the other hand, a small part of these sediments may come from the surface runoff associated with rainfall events, from aeolian processes, or from authigenic processes [23–26,29].

Some previous studies in Mallorca caves reported the presence of allochthonous sediments whose provenance from the island was questioned due to the purity of the bedrock materials and the fact that there are not outcrops with sufficient quantities of quartz, feldspar, and clay minerals in the island [25,26]. The X-ray diffraction study performed by Fornós et al. [30] indicated that these minerals were, in fact, directly related to the dust material from the Sahara that reaches the island in the form of mud rain.

In any case, in order to have a better understanding of the origin (autochthonous or allochthonous) of the sediments inside the caves, extensive studies of the clay minerals in those sediments and in the bedrock and the soil outside the cave, are needed [4,31]. For this reason, we carried out a combined grain size and clay mineralogical analysis by means of

X-ray diffraction and electron microscopy of the sedimentary deposits included in the Ases cave (eastern Mallorca). The three main aims were: (1) to classify the cave deposits from a sedimentological point of view and determine their provenance and paleoenvironmental significance; (2) to determine the origin (authigenic vs. detrital) of the clay minerals included in the cave deposits; and (3) to examine the mineralogical variations through the different conduits of the cave, especially the clay mineral fraction, in order to establish the paleoenvironmental conditions inside the cave over time.

2. Geological and Geographical Setting

The Mallorca Island, located on the western Mediterranean Sea, is the largest island in the Balearic archipelago (Figure 1). There are a large number of caves all along the coast of the island and the most important and most studied cavities are part of the karstic region called “Marina de Llevant” formed by a post-orogenic tabular platform composed of Tortonian-Messinian calcarenites and reef limestones (Figure 1) [32]. These kinds of caves present features related to phreatic dissolution in the mixing zone between fresh and marine waters, and currently some parts of these caves are submerged under brackish waters, resulting in subterranean pools, where the water table movements are controlled by the sea level [33].

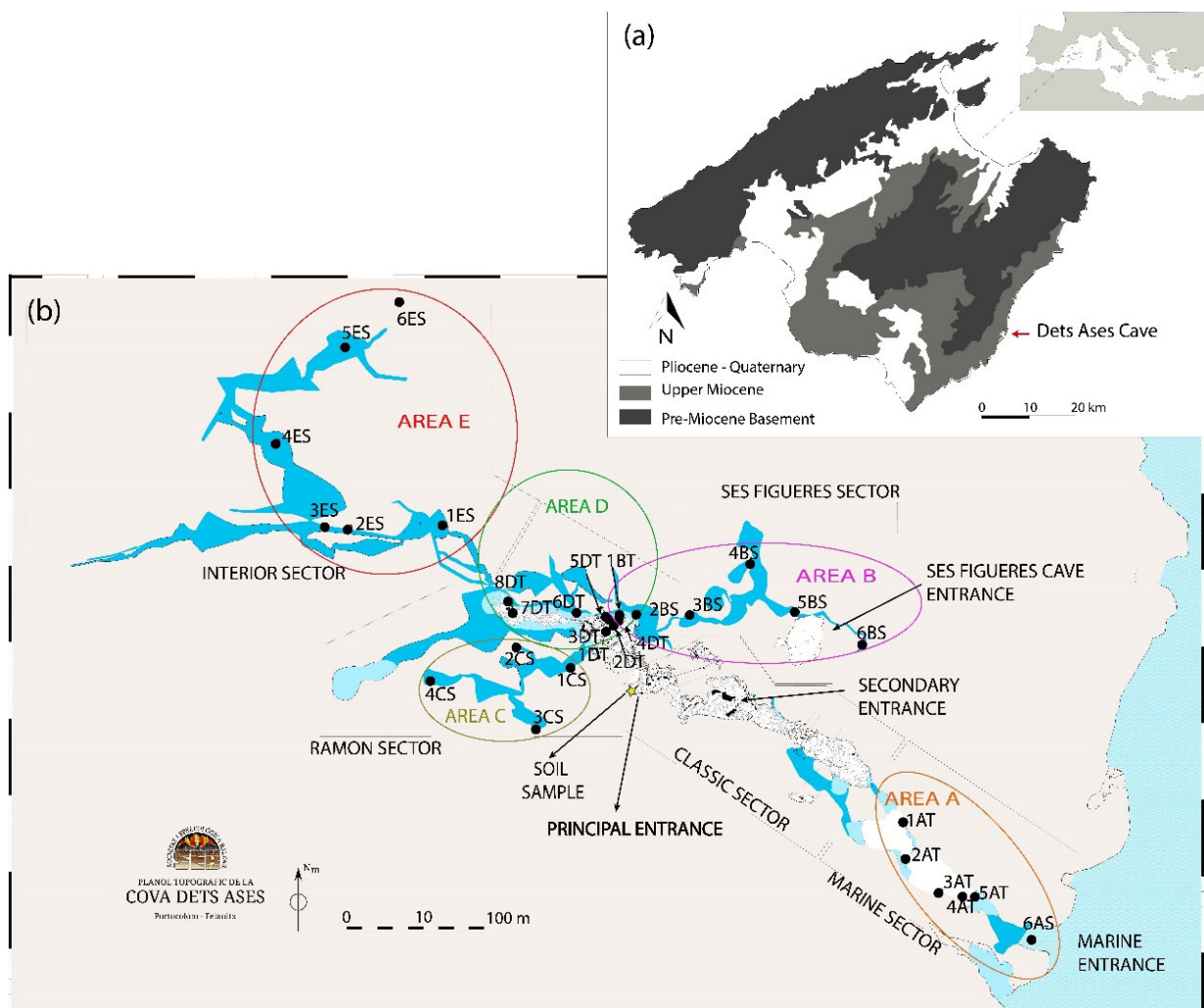


Figure 1. (a) Simplified geological map of the Mallorca Island in the western Mediterranean Sea showing the location of the Ases cave on the east coast (modified from Tuccimei et al. [33]); (b) Ases cave map with the different sectors of the cavity and areas where the samples have been taken (Societat Espeleològica Balear, unpublished).

The karstification processes in this area started during the Upper Miocene due to the dissolution of the carbonate materials [32,34], followed by the development of protocavities in the marine-meteoric water mixing zone. The fluctuations of the sea level generated instabilities and mechanical readjustments that caused the subsidence and collapse that resulted in large cavity rooms [22,35]. During the Upper and Middle Pleistocene, speleogenetic processes were dominated by the precipitation of vadose and phreatic speleothems and by the deposition of detrital materials with different origins inside the caves [34]. The principal development of these cavities is horizontal with the alternation of underwater, vadose, and/or terrestrial zones [35]. This close relation with the sea level inside of the coastal cavities leads to the development of hypogean lakes with anchialine environments of great scientific interest, such as the relatively new and very strange deposits known as Phreatic overgrowths on speleothems (POS) [22,23,33,36]. Additionally, the most important climatic factor since the formation of the caves to the present is the variation of the Mediterranean sea level. During the glacial periods, i.e., cold and dry, the Mediterranean sea level was low, while during the interglacial epochs, associated to humid and warm periods, the sea levels were high.

Most of the sedimentary deposits inside the Mallorca caves can be separated in 2 groups following the classification of Bosch and White [18], based on the type of water flow and energy responsible for generation [24,25,27]:

- (1) Backswamp facies, which consist of fine material from the residue of the bedrock weathering (carbonates) together with a small part of infiltrated material from the soil outside the cave. The deposits that proceed from the bedrock weathering are considered autochthonous deposits whereas the small quantities derived from the infiltrated materials are considered allochthonous.
- (2) Slackwater facies, which consist of fine-grained reddish clayey silts, located in the ground and in the bottom of the lakes, whose composition is characterized mainly by quartz, feldspar, and clay minerals, although they also contain some carbonates. These materials come from the surface and enter into the caves by the runoff associated with rainfall events [26]. Therefore, these deposits have an allochthonous origin.

Although slightly less common, Fornós et al. [37] defined a third group of sediments in Mallorca, the so called “Reddish silts and clay”. This group includes red clay and fine-grained sediments found filling holes in the walls and bottoms of the cave. Their input seems to be related to transport in suspension in a water flow. These deposits were described in Sa Gleda cave [26], and Coll cave (Cova des Coll) [24], where some evidence of erosion was also observed indicating that they are associated to earlier stages of filling and subsequent emptying of the cavities.

The Ases cave is a coastal cave located on the east coast of the island (Figure 1), close to Portocolom village (Felanitx municipality), 500 m away from the S’Algar beach [38]. There are three entrances to the cave known so far, two terrestrial and one submarine (Figure 1). The still ongoing cartographic studies in the underwater part might discover additional entrances.

The Ases cave develops in the general direction SE-NW from the principal entrance although there are some additional developments in a more or less perpendicular direction, NE-SW (Figure 1) [32]. The deposits found inside this cave have been initially separated into terrestrial and submarine, although a more detailed classification will be presented below. The samples have been collected in five areas (A, B, C, D, and E), and they are included in the different sectors of the cave (Figure 1):

- (1) Area A corresponds to Marine sector on the survey of the cave and presents a SE-NW direction. It has a total development of 275 m; 105 m of them underwater and with a direct submarine connection to the sea and 170 m of terrestrial development. Five samples were taken on the terrestrial part of this area and another on the submerged part closed to the entrance of the cave (Figure 1).
- (2) Area B corresponds to Ses Figueres sector with a NE-SW general direction. The Ses Figueres cave, located on this sector, was considered in the past as an independent

cavity with its own terrestrial entrance, but the recent underwater topography works have revealed that there is underwater communication with the main Ases cave. The development of this sector has 75 m terrestrial, where one sample was taken, and 340 m underwater, where five samples were taken.

- (3) Area C is located on the NE-SW site of the Ramon sector and is completely submerged. The entire Ramon sector (separated in NE-SW part, associated to area C, and SE-NW part, associated to area D) has the greatest development with the existence of several lakes far from the coast. All the sector discovered so far consists of 240 m of terrestrial development and 555 m underwater. Four submerged samples were taken on this area.
- (4) Area D corresponds with SE-NW site of the Ramon sector and with more terrestrial development, a total of eight terrestrial samples were taken on this area.
- (5) Area E corresponds to Interior sector and develops underwater with a SE-NW general direction and the still ongoing mapping has discovered more than 300 m of submarine to date. Six submerged samples have been collected in this area.

The Classic sector, where no samples were collected here for this study due to the tight schedule of the sampling campaigns, was first mapped in 1972 [32,38], develops along 340 m towards the NW. It is a terrestrial part of the cave where the principal and second terrestrial entrances are located.

It is expected that the ongoing survey works will modify the final aspect of this map, including the names and extension of the sectors defined so far.

3. Materials and Methods

The sediment samples were collected during several fieldwork campaigns inside the cavity. The sampling sites were selected trying to cover the entire mapped cavity (considering the difficulty in some points) and to get representative information of the terrestrial and subaqueous parts.

The samples were studied at the laboratories of the Universities of the Balearic Islands and of Zaragoza. To characterize the sediments present in Ases cave, the color and the grain size were determined, the organic matter fraction was calculated, and a mineralogical study, by means of X-ray diffraction and electron microscopy, was carried out.

3.1. Sampling of the Cave Sedimentary Deposits

A total of 32 samples were collected inside the Ases cave (Figure 1). They were taken from terrestrial and submerged zones and at different distances from the different entrances. This distribution was intended to provide the necessary information to understand the possible different mineralogical, morphological, or grain size distribution and from that, to allow recognizing the possible sedimentary processes that have affected the cavity. From these 32 samples, 14 of them correspond to the terrestrial sediments of the cave (hereinafter referred to as terrestrial samples), 16 come from underwater sediments (hereinafter referred to as submerged samples), 1 is from the bedrock (constituted by Tortonian-Messinian calcarenites), and 1 has been collected in a soil at the main entrance of the cavity. The soil sample was taken from the O horizon, the most superficial part of a soil which, in this case, is directly underlined by the bedrock (R layer). This implies the poor development of the soil horizons in this zone.

The labels of the samples consist of a number (increasing from the terrestrial cave main entrance towards the interior or towards the see in the case of Area A), the area letter, and a T for the terrestrial samples or an S for the submerged samples. The distribution of the samples in the cave covers almost the entire area mapped until 2022 (Figure 1).

The sediments inside the cave have been found on the floor of the submerged galleries and rooms and filling the voids in walls or ceilings in the emerged areas. The sediments deposited in the floor under the water between 3 and 10 m depth are formed by vertical accumulation of material, while the ones in the ceilings and walls at heights between 0.5 and 2.5 m in the terrestrial areas are fillings embedded in small holes within the bedrock.

The sample collection was made using 50 mL Falcon tubes. These tubes were inserted into the deposit, extracted, closed, and maintained in the fridge until they were analyzed in the laboratory.

3.2. *Drying of the Samples and Determination of Color and Organic Matter*

The humidity of the samples was removed by heating them in an Argolab TCN 115 Plus oven at 105 °C for 24 h. The color of the samples was determined by using the Munsell system in each sample before and after drying. This methodology consists of the visual comparison of the samples studied with the reference colors by the Munsell® soil color charts [39]. The organic matter content was measured in a portion of all the samples by using the weight loss value after the sample calcination in a Carbolite ELF 11/6B muffle at 500 °C during 24 h.

3.3. *Grain Size Analysis*

The particle size distribution was determined using a Mastersizer 2000 laser granulometer. The statistical analysis of the data was performed with the Gradistat (v 8.0) program by the Logarithmic Folk and Ward [39] method of analysis obtaining cumulative curves, frequency histograms, and statistical data [40]. Grain size analyses were performed in all the samples collected inside the cavity with the exception of the bedrock sample (Bedrock), which was not analyzed. Finally, two analyses in duplicate were performed using the sample from the soil (Soil) outside the main entrance to have a more representative value.

3.4. *X-ray Diffraction Study*

The 32 sediment samples were studied by X-ray diffraction (XRD) in order to determine their mineralogical composition. The bedrock sample was crushed before the analysis. To obtain the diffraction patterns, a Bruker D8-Advance X-ray diffractometer at the University of Balearic Island, with 40 kV voltage, 40 mA current, CuK α radiation was used. The XRD patterns were acquired from 3 to 70° 2 θ . The step size was 0.020 and the time per step 96 s. The XDR patterns were calculated with the Diffrac Suite EVA v. 4.4 software.

The <2 μ m fractions were extracted by centrifugation and analyzed in air-dried and ethylene-glycol-treated oriented aggregates to determine the clay minerals present in the samples. To obtain the <2 μ m fractions diffraction patterns, a Philips 1710 diffractometer was used at the University of Zaragoza, with 40 kV voltage, 30 mA current, CuK α radiation, an automatic slit, and a graphite monochromator. The XRD patterns in this case were acquired from 3 to 30° 2 θ .

Once the mineral phases present in the whole rock and the <2 μ m fractions were determined, the relative proportions of these mineral phases were obtained. The relative proportions in the whole rock XRD patterns were calculated with Diffrac EVA v.7.0 software. In the <2 μ m fractions the relative proportions were acquired using Reference Intensity Ratio (RIR) from the literature [41]. The full width at half maximum (FWHM) of the 001 reflections of kaolinite in the air-dried oriented aggregates was measured to determine kaolinite crystallinity in order to estimate the crystallization conditions of this mineral.

3.5. *Electron Microscopy Study (SEM)*

Once the minerals phases present in the sediment samples were determined, fragments of six samples (three from terrestrial and three from submerged sediments) were selected for the electron microscopy study to determine micro textural differences between them. The soil sample was also observed under electron microscopy to compare its texture with that of the cave sediments.

Morphological images and mineralogical information of the samples were obtained by using a Carl Zeiss Merlin field emission scanning electron microscope (FESEM) equipped with an Oxford energy-dispersive X-ray (EDS) detector. For this, the sediments fragments and the soil sample were previously kept under vacuum conditions for 24 h and carbon-

coated, and a secondary electron detector (In-lens) was used. The accelerating voltage was 5 kV with a beam current of 100 pA.

4. Results

4.1. Color and Organic Matter Content

The differences in color found between the wet and the dry samples are compiled in Table 1. The general color in all the samples is reddish with orange tones and it becomes darker when the samples are dry.

Table 1. Color for the wet and dry samples according to the Munsell System and organic matter content in all the studied samples.

	Sample	Wet Color	Dry Color	Org Mat (%)		Sample	Wet Color	Dry Color	Org Mat (%)
Area A	1AT	10 R 2.5/2	10 R 2.5/1	3.6	Area B	1BT	10 R 4/6	2.5 YR 4/6	2.4
	2AT	2.5 YR 2.5/4	2.5 YR 3/6	4.5		2BS	10 YR 6/8	7.5 YR 6/8	2.1
	3AT	2.5 YR 3/6	2.5 YR 3/6	3.8		3BS	7.5 YR 4/6	10 YR 6/6	2.6
	4AT	10 YR 6/6	10 YR 6/7/4	1.3		4BS	5 YR 5/8	7.5 YR 5/8	2.3
	5AT	2.5 YR 3/6	2.5 YR 2.5/4	4.0		5BS	5 YR 4/6	7.5 8/4	2.0
	6AS	10 YR 5/8	2.5 YR 3/6	5.2		6BS	2.5 YR 4/8	5 YR 4/6	5.0
	Sample	Wet Color	Dry Color	Org Mat (%)		Sample	Wet Color	Dry Color	Org Mat (%)
Area C	1CS	7.5 YR 5/8	7.5 YR 7/8	4.6	Area D	1DT	10 R 3/6	2.5 YR 4/8	5.3
	2CS	10 YR 7/6	10 YR 8/4	2.9		2DT	1 for gley 5/5G	2.5 YR 8/2	1.2
	3CS	7.5 YR 6/8	7.5 YR 8/6	4.2		3DT	7.5 YR 8/4	10 YR 8/2	1.7
	4CS	5 YR 4/6	5 YR 3/4	5.5		4DT	2.5Y 7/2	2.5 Y 8/2	3.8
	Sample	Wet Color	Dry Color	Org mat (%)		Sample	Wet Color	Dry Color	Org Mat (%)
Area E	1ES	2.5 YR 4/8	2.5 YR 4/6	24.0	Area D	5DT	10 R 3/6	10 R 3/6	4.5
	2ES	5 YR 5/8	5 YR 4/6	3.3		6DT	10 R 3/3	10 R 3/4	3.3
	3ES	5 YR 4/6	7.5 YR 4/6	3.3		7DT	10 R 4/6	10 R 4/8	4.7
	4ES	7.5 YR 5/8	10 YR 6/8	2.0		8DT	10 R 3/6	10 R 3/6	4.2
	5ES	7.5 YR 5/6	7.5 YR 5/6	4.9		Soil	7.5 YR 3/1	7.5 YR 3/2	19.2
	6ES	2.5 YR 4/8	5 YR 4/6	0.9					

The average organic matter percentage of all samples is 4.10%, but the soil sample and the sample 1ES (area E) have the highest values (19.16% and 24.02%, respectively). The average for the submerged samples is 4.68%, while for the terrestrial samples it is 3.45% (without Soil sample), there is not a significant difference in their organic matter content.

4.2. Grain Size Results

All samples (Table 2 and Table S3 in Supplementary Materials) have a 3.9 mean (Mz) and a 3.5 ϕ median (D₅₀). The sorting is “Very Poorly Sorted” with a value of 2.5. Most of samples show a positive skewness, with a value of 0.2 and a preferential development to the left of the means and are classified as Fine Skewed. The mean kurtosis in all samples is 0.9, which corresponds to a mesokurtic morphology.

The terrestrial samples (Table 2 and Table S3 in Supplementary Materials) have a 4.2 mean (Mz) and a 3.6 ϕ median (D₅₀). The sorting is “Very Poorly Sorted” with a 2.8 value; the samples skewness is positive, with a value of 0.3, and it is classified as fine skewed. The mean kurtosis value is 0.9, corresponding to a mesokurtic morphology.

The submerged samples (Table 2 and Table S3 in Supplementary Materials) show very similar values. They have the same mean value as the terrestrial samples (4.2 Mz) although a slightly higher median value (4.0 ϕ ; D₅₀). Their sorting is also “Very Poorly Sorted” (2.5) and the skewness positive (0.2) with left development. It also corresponds to fine skewed

and with a 1.0 kurtosis value, associated, like in the case of the terrestrial samples, with mesokurtic morphologies.

Table 2. Average particle size data for all samples (including the two soil samples), terrestrial and submerged samples.

	All Samples	Terrestrial Samples	Submerged Samples
Mean	3.90	4.20	4.20
Sorting	2.50	2.80	2.50
Skewness	0.20	0.30	0.20
Kurtosis	0.90	0.90	1.00
D₅₀ (φ):	3.5	3.6	4.0

The grain size results have been classified according to class weight (%) versus the particle diameter (μm), obtaining 5 main classes (Figure 2 and Table 3). Class 1 represent unimodal populations with the maximum size lower than 100 μm (Figure 2, sample 3BS). Class 2 samples show also a unimodal distribution, but the maximum size is equal or higher than 100 μm (Figure 2 sample 5BS). Class 3 samples show bimodal populations in which the largest grain sizes (between 50 and 1000 μm particle diameter) represent the largest population (Figure 2 sample 3CS). Class 4 also show a bimodal distribution but in these samples the largest population contains the samples with the smallest size (between 1 and 50 μm; Figure 2 sample 1AT). Finally, the polymodal samples are included in Class 5 and are associated with various particle size populations (Figure 2 sample 5ES).

Table 3. Relationship between the samples of each area, the sample type, the grain size distribution and the sample Class.

	Sample Type	Class		Sample Type	Class
	Area A			Area B	
1AT	Bimodal	4	1BT	Bimodal	3
2AT	Bimodal	3	2BS	Trimodal	5
3AT	Unimodal	2	3BS	Unimodal	1
4AT	Bimodal	3	4BS	Unimodal	1
5AT	Unimodal	2	5BS	Unimodal	2
6AS	Unimodal	2	6BS	Bimodal	3
	Area C			Area D	
1CS	Bimodal	3	1DT	Bimodal	3
2CS	Bimodal	3	2DT	Unimodal	2
3CS	Bimodal	3	3DT	Unimodal	2
4CS	Unimodal	2	4DT	Bimodal	3
	Area E		5DT	Trimodal	5
1ES	Polymodal	5	6DT	Bimodal	4
2ES	Unimodal	1	7DT	Bimodal	3
3ES	Bimodal	4	8DT	Bimodal	3
4ES	Bimodal	4	Soil A	Unimodal	2
5ES	Polymodal	5	Soil B	Unimodal	2
6ES	Trimodal	5			

The specific class for each sample is indicated in Table 3. In total, from the 32 samples in which this grain size study was performed, 12 are unimodal, 15 are bimodal, and 5 polymodal (Table 3). Considering the type of the sample (Table 4), from the 14 terrestrial sediment samples, 9 are bimodal (7 are Class 3 and 2 are Class 4), 4 are unimodal (Class 2), and 1 sample is polymodal (Class 5). In the case of the 16 submerged samples, 6 of them are

unimodal (3 are Class 1 and 3 are Class 2), 6 are bimodal (4 of them Class 3 and 2 of them Class 4), and Class 5 is formed by 4 polymodal samples. The other 2 samples correspond to the soil samples and are unimodal, Class 2.

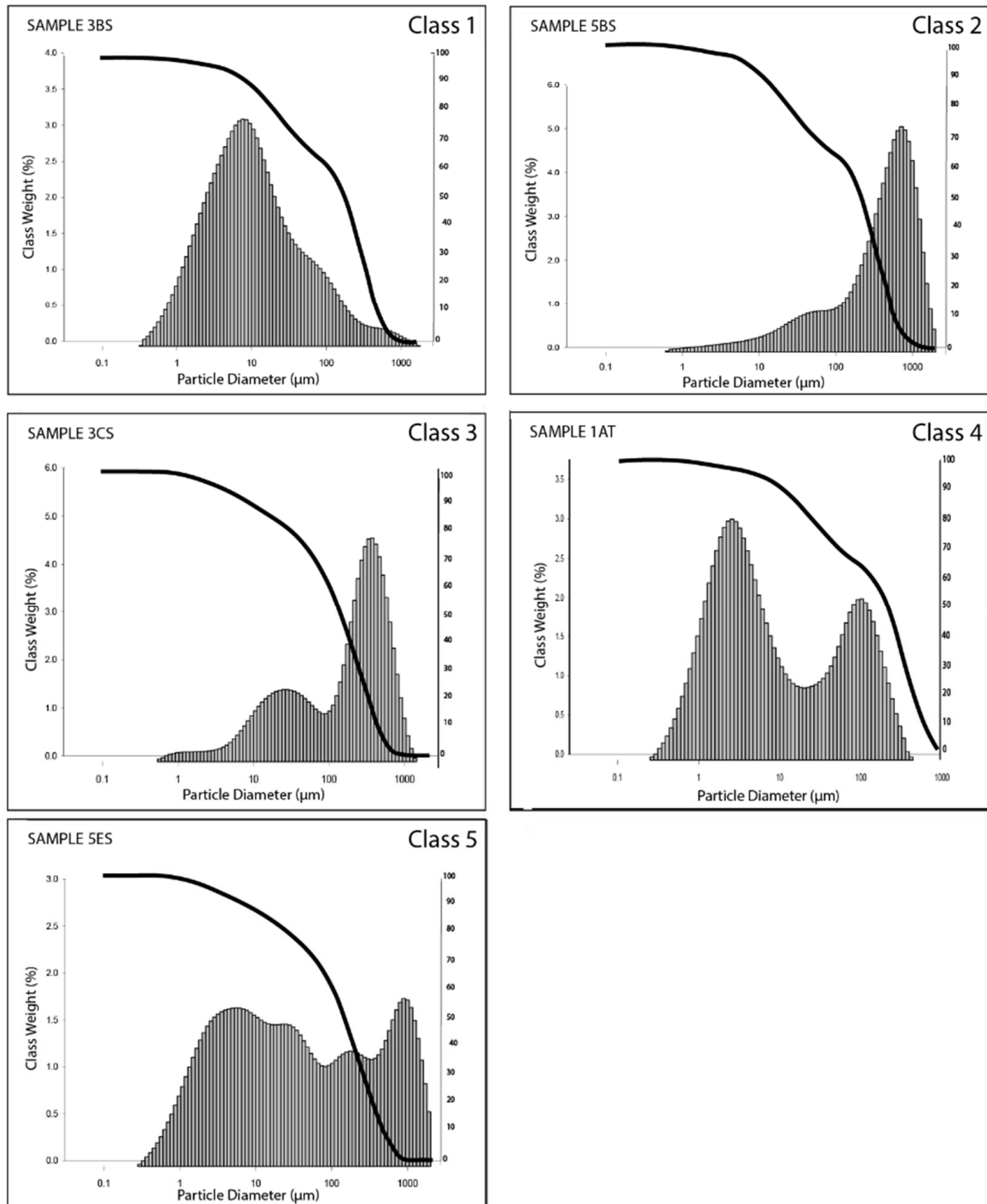


Figure 2. Grain size cumulative curve and frequency histogram of some samples of sediments in Ase cave representative of the five differentiated classes. (1) Sample 3BS: submerged and unimodal sample, Class 1. (2) Sample 5BS: submerged and unimodal sample, Class 2. (3) Sample 3CS: submerged and bimodal sample, Class 3. (4) Sample 1AD: terrestrial and bimodal sample, Class 4. (5) Sample 5ES: submerged and polymodal sample, Class 5.

Table 4. Relation between the terrestrial and the submerged samples with their class.

	Unimodal		Bimodal		Polymodal	Total of Samples
	Class 1	Class 2	Class 3	Class 4	Class 5	
Terrestrial		4	7	2	1	14
Submerged	3	3	4	2	4	16

The average grain size composition of the samples is 0.4% gravel, 55.6% sand, and 44% mud (Table 5). The terrestrial samples are constituted by 0.5% gravel, 57.9% sand, and 41.5% mud; and the submerged samples by 0.2% gravel, 49.8% sand, and 50.1% mud (Table 5).

Table 5. Gran size composition of each studied sample and average values for the terrestrial and the submerged groups.

	Area A						Area B					
	1AT	2AT	3AT	4AT	5AT	6AT	1BT	2BS	3BS	4BS	5BS	6BS
% Gravel	0.0	0.0	0.1	6.2	0.0	0.0	0.3	0.1	0.0	0.0	0.2	0.0
% Sand	23.0	60.4	63.8	93.8	56.5	69.7	53.7	69.9	13.9	37.4	84.1	53.7
% Mud	77.0	39.6	36.2	0.0	43.5	30.3	46.0	30.0	86.1	62.6	15.7	46.3
	Area C						Area D					
	1CS	2CS	3CS	4CS	1DT	2DT	3DT	4DT	5DT	6DT	7DT	8DT
% Gravel	0.0	0.1	0.0	0.5	0.00	0.00	0.00	0.00	0.00	0.00	0.00	0.00
% Sand	77.0	70.8	68.4	79.7	0.58	0.55	0.74	0.57	0.57	0.33	0.67	0.57
% Mud	23.0	29.1	31.6	19.7	0.42	0.45	0.26	0.42	0.43	0.67	0.33	0.42
	Area E						Terrestrial average	Submerged average				
	1ES	2ES	3ES	4ES	5ES	6ES						
% Gravel	0.2	0.0	0.2	0.7	0.3	0.2	0.5	0.2				
% Sand	39.1	8.4	21.8	35.6	40.5	26.2	57.9	49.8				
% Mud	60.7	91.6	78.0	63.7	59.2	73.6	41.5	50.1				

Considering the location of the studied samples in the different areas of the cave, the results indicate that the areas A, B, C, and D have a higher proportion of sand, while the area E, the deepest and farthest from all the entrances, has a higher proportion of mud. Some other interesting observations are related to two specific samples, 4AT and 5BS. The first one has the highest gravel and sand concentration (gravel 6.2% and sand 93.8%) and the second also shows a very high sand percentage (84.1%). In both cases, this important percentage of large grain sediments is associated to the proximity to the entrances, the submarine one in the case of 4AT and the Ses Figueres cave entrance in the case of 5BS. In general, the terrestrial samples present more sand, and the submerged samples have more mud material.

4.3. X-ray Diffraction Mineralogy

The mineralogical study of the samples by X-ray diffraction was conducted in 2 phases, the first one determined the mineralogy of the whole sample and the second phase focused on the study of the <2 μm fraction of the samples to analyze the clay fraction.

4.3.1. Whole Sediment and <2 μm Fraction Mineralogy

The XRD results of the whole sediment samples of the Ases cave show that they are mainly formed by clay minerals, calcite, and quartz, together with minor proportions of dolomite, albite, orthoclase, hematite, and goethite (Table S1 in Supplementary Materials). The soil sample is mainly formed by quartz (45%), clay minerals (32%) and calcite (20%) together with minor proportions of orthoclase and goethite (<5%). The bedrock sample is

mainly constituted by calcite (97%) with minor proportions of quartz and clay minerals (<5%). Among the clay minerals, kaolinite and illitic phases were identified.

Overall, the submerged samples have higher calcite (38%) and quartz (28%) content than the terrestrial samples (calcite = 20% and quartz = 12%), but lower clay minerals content (31% versus 60%). The “illitic phases” (this term includes illite polytypes and micas species and are quantified together) are the dominant clay minerals in all the samples (20%–38%) followed by kaolinite, whose content is higher in the terrestrial samples (15% versus 6%). Small quantities of chlorite are also detected in terrestrial (~9%) and submerged (<5%) samples, whilst small proportions of smectite (<5%) are only detected in the submerged samples.

Regarding the clay minerals in the soil and the bedrock samples, the illitic phases are the dominant clay minerals (23%) and kaolinite is also identified (8%). Neither smectite nor chlorite are identified in the soil or in the bedrock samples (Figure 3).

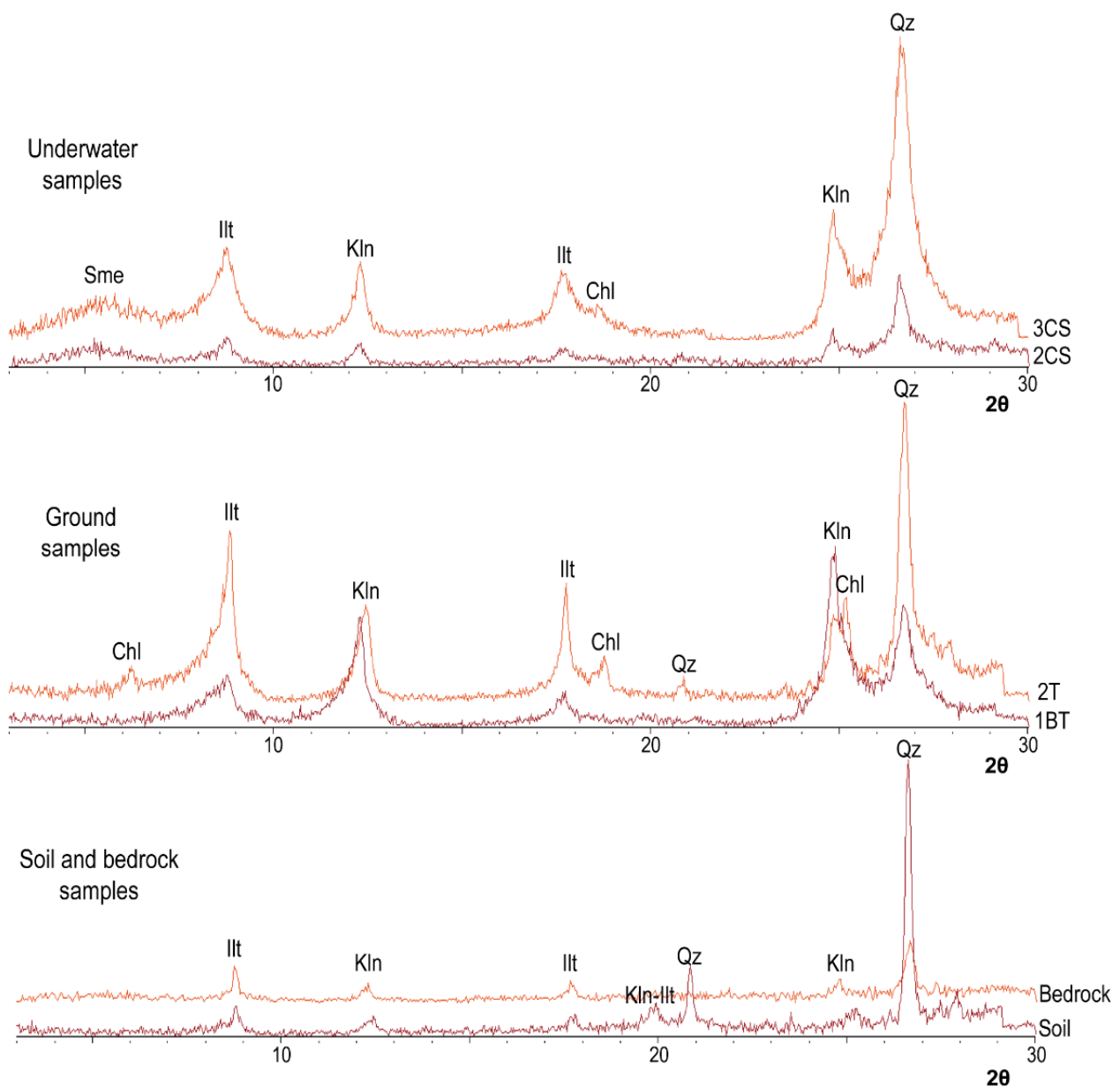


Figure 3. Representative XRD patterns obtained from the <2 μm fractions in submerged samples, terrestrial samples, the bedrock and the soil samples. Qz = Quartz; Illt = Illitic phases; Kln = Kaolinite, Chl = Chlorite; Sme = Smectite.

In the XRD patterns of the $<2 \mu\text{m}$ fraction, the clays identified are the same as mentioned above: kaolinite (7 Å), illitic phases (10 Å), chlorite (14 Å), and smectite (15 Å) (Figure 3) in both types of samples, while smectite is only detected in the submerged ones (Figure 3).

4.3.2. Mineralogical Trends Inside the Cave

Quartz is the main phase in the area E, the inner sector, and its content decreases towards the entrance of the cave. Conversely, illitic phases and kaolinite are dominant in area A and the contents of hematite, goethite, orthoclase, and albite are also higher in this area. The content of all these minerals decreases towards the interior of the cave. Finally, the calcite content is higher in the sectors developed perpendicular to the main cave direction, the areas B and C. The relative proportions of the mineral phases included in the sediments collected in the different areas of the Ases cave are summarized in Figure 4. In each area, two groups of samples have been separated according to their carbonate content and their results are shown in two different bars (Figure 4).

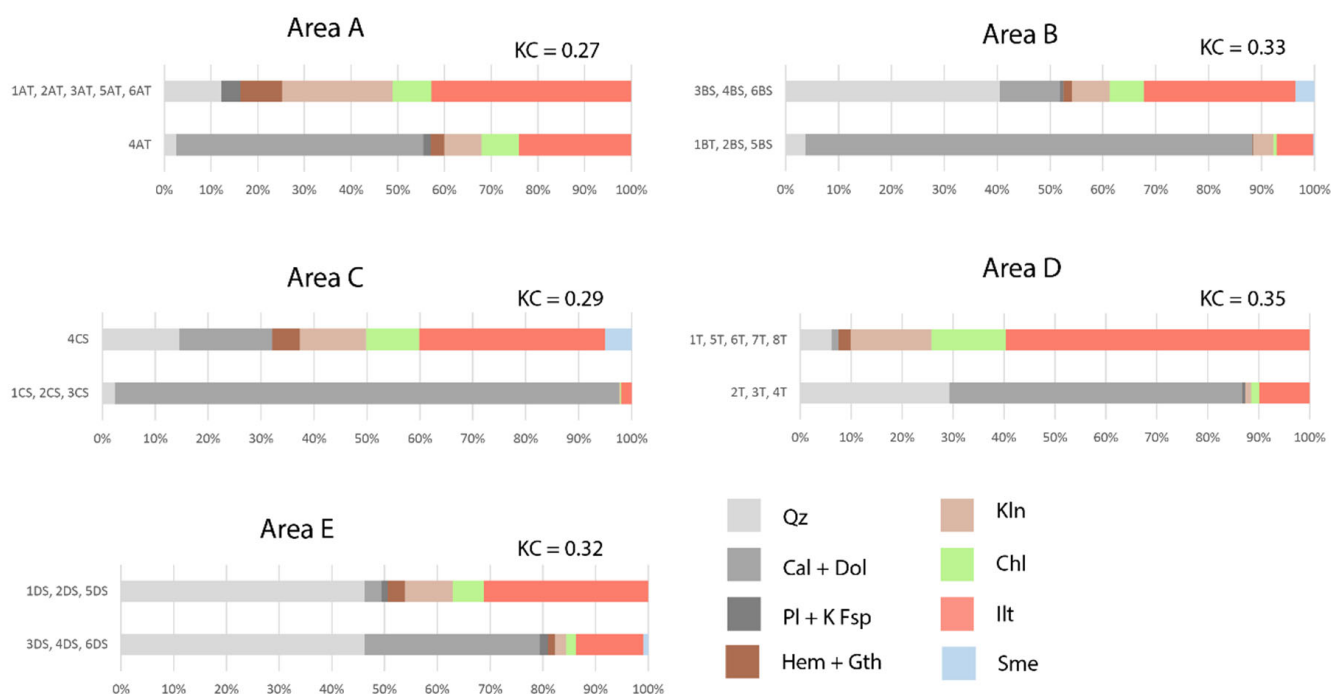


Figure 4. Average of the relative proportions of the mineral phases present in the samples from each area of the cave. The diagrams for each area include two horizontal bars representing samples with high and low carbonate content. The average value of kaolinite crystallinity (KC) in each area is also indicated. Lower values indicate higher kaolinite crystallinity, and viceversa. Qz = Quartz; Cal = Calcite; Dol = Dolomite; Pl = Plagioclase; K Fsp = Potassium Feldspar; Hem = Hematite; Gth = Goethite; Kln = Kaolinite; Chl = Chlorite; Illt = Illitic Phases; Sme = Smectite.

The average values for the kaolinite crystallinity are also indicated in Figure 4 and the kaolinite crystallinity value of each sample is included in Table S2 (Supplementary Materials). According to these data, kaolinite is more crystalline in area A, where its content is higher. Its crystallinity decreases in the rest of the areas, coinciding with the decrease in this mineral content towards the interior of the cave. The lowest kaolinite crystallinity is recorded in area D, where kaolinite content is higher than in areas B, C, and E. Finally, kaolinite is more crystalline in the bedrock sample (0.12) than in the soil sample (0.37) (Table S2).

4.4. Electron Microscopy Results

The secondary electron images of the samples confirm that the clay minerals included in the terrestrial and the submerged samples, as well as in the soil sample, are mainly kaolinite and illitic phases (Figures 5 and 6).

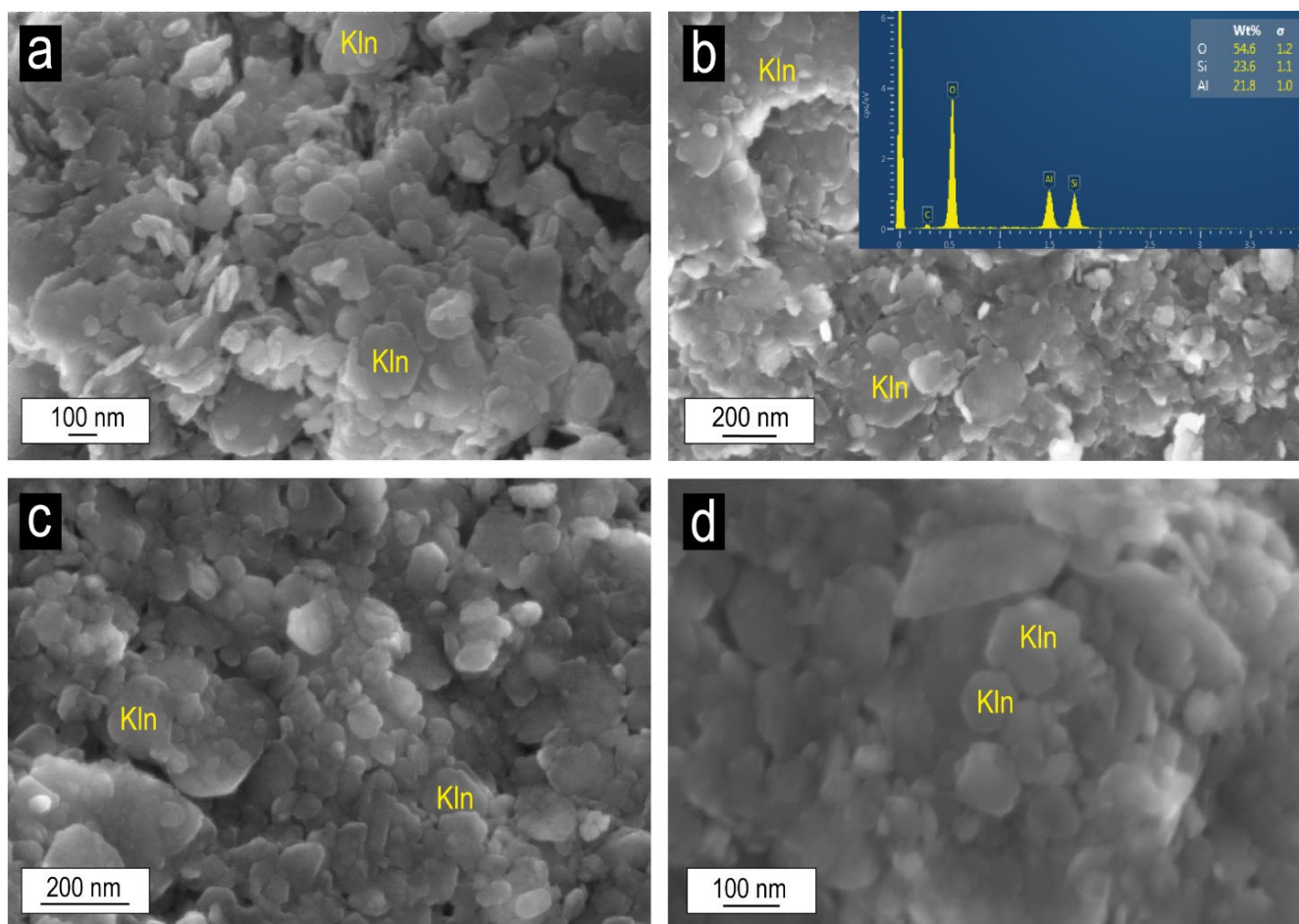


Figure 5. Secondary electron microscopy images of terrestrial (a,b) and submerged (c,d) samples showing subeuhedral to euhedral kaolinite plates occasionally displaying hexagonal outlines. Kln = kaolinite. Figure 5b includes an EDS pattern of kaolinite from the terrestrial samples.

Kaolinite appears in general as nanometric-size subeuhedral to euhedral plates with random orientation in both terrestrial (Figure 5a,d) and submerged samples (Figure 5c,d). The illitic phases are heterometric (500 nm–3 μ m) but with higher sizes than the kaolinite plates (Figure 6a–c). They appear as plates (Figure 6a,b) or with anhedral and wavy morphologies (Figure 6c) in both types of samples. Kaolinite is frequently observed over the illitic phase plates (Figure 6a). Smectite is also observed in certain submerged samples with flake morphologies (Figure 6d), especially in those located in the medium parts of the cave (areas B and C).

In the soil sample, the illitic phases appear as heterometric plates with the same sizes than those included in the samples from inside the cave (Figure 6e). By contrast, kaolinite from the soil sample presents platy morphologies but with anhedral outlines (Figure 6f).

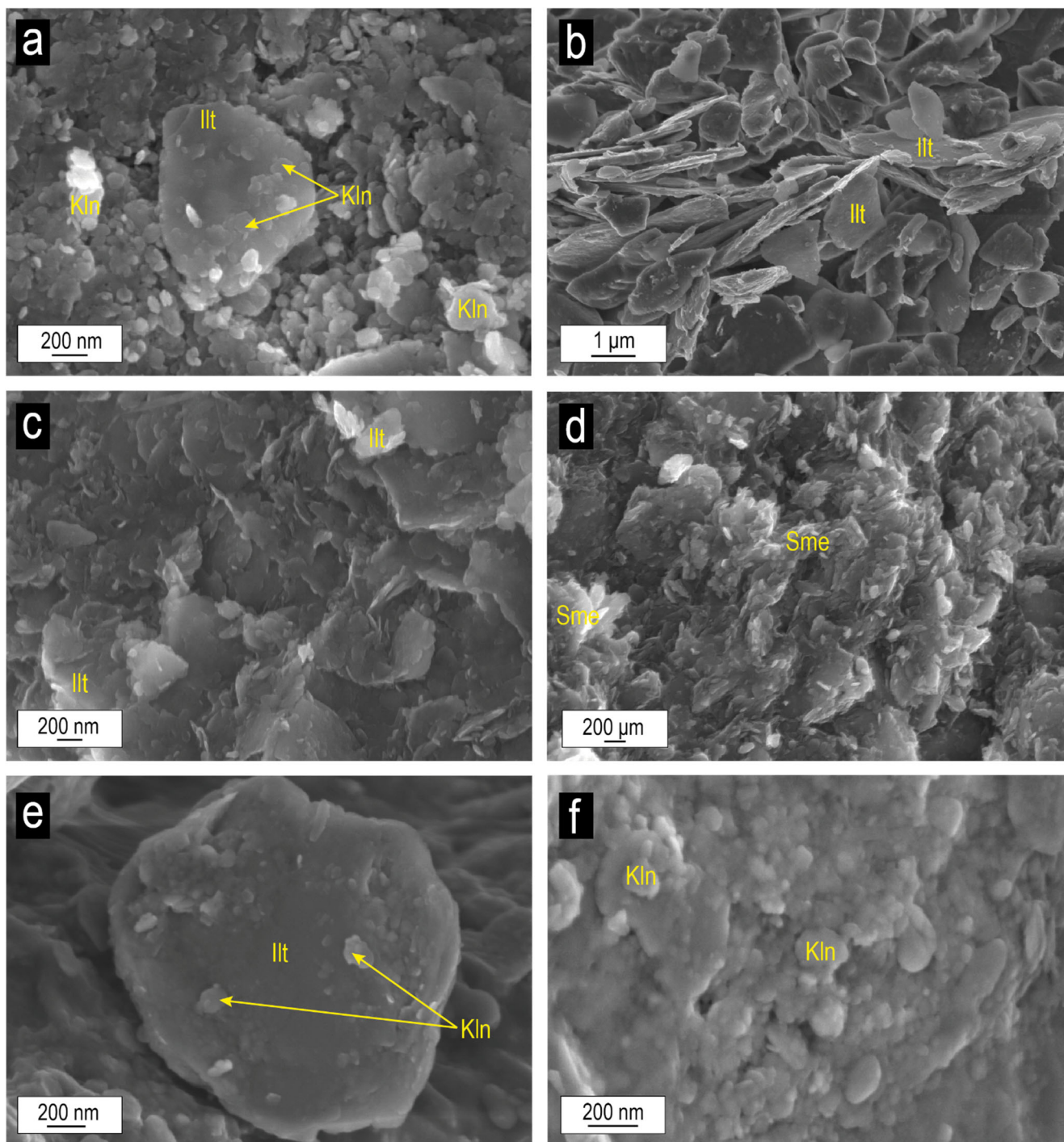


Figure 6. Secondary electron images showing: (a) illitic phases plates with anhedral morphologies and subhedral kaolinite plates in terrestrial samples; (b) illitic phases plates with anhedral morphologies in terrestrial samples; (c) illitic phases with wavy morphologies in submerged samples and EDS patterns of the illitic phases; (d) smectite with flake morphologies in submerged samples and EDS patterns of smectite; (e) illitic phases plates with anhedral morphologies and anhedral kaolinite plates in the soil sample; (f) anhedral kaolinite plates in the soil sample. Kln = Kaolinite; Illt = Illitic phases; Sme = Smectite.

5. Discussion

5.1. Grain Size Distribution

As mentioned before, the grain size analysis shows that all samples are very poorly sorted, with a positive skewness, mesokurtik morphology, fine skewed. Terrestrial and submerged samples present the same mean values, but these values are different from the global mean since this last also includes the two soil samples. By contrast, the median values are different for the terrestrial (3.6 ϕ) and for the submerged samples (4.0 ϕ).

The study of the grain size allowed the classification of samples as unimodal, bimodal and polymodal depending on the number of grain-size populations in each sample. Following the works of Blott and Pye [40] and Visher [42], five classes have been differentiated and they can be related to the different sedimentary processes that take place around the cave conduits and halls (Figure 2 and Table 6):

- (1) Class 1. It is formed by unimodal samples characterized by small particle size and they may be associated to the movement of suspension material [37,40,42]. It is only found in the submerged sediments (Table 4).
- (2) Class 2. It is constituted also by unimodal samples but with larger particle sizes. These samples may be related to different processes: (a) material arrival by saltation or creep, in the samples with low proportions of calcite; (b) bedrock erosion, weathering, and/or degradation processes [24,25,27,37], allowing the accumulation of carbonate material mixed with sand and clay at the bottom of the pools; that would be the case of the samples with high calcite proportions; and (c) fall of floating calcite and accumulation at the bottom of the pools [24,25,27], although this process can be discarded because the deposits did not show the typical floating calcite morphologies.
- (3) Class 3. It is constituted by bimodal samples with two different populations of particle size. Like in the previous classes 1 and 2, the population with the small grain size would be related with the movement of fine particles in suspension, while the population with the large size would be with the saltation or creep mechanism, or the bedrock erosion. The large size population is the dominant in this class and more sediments from the terrestrial than from the submerged group belong to this class 3.
- (4) Class 4. It is similar to Class 3, although the dominant population in this bimodal distribution is the small grain size population. The processes associated to the populations would be the same as the ones mentioned above. It seems to be equally common in the terrestrial and in the submerged sediments (Table 4).
- (5) Class 5. It is constituted by polymodal samples which are most likely related with superposition of different sedimentary processes (suspension, saltation or creep and weathering of bedrock). This kind of distribution seems to be more common in the submerged sediments than in the terrestrial ones.

5.2. Mineralogical and Sedimentary Trends in the Conduits of the Cave

As indicated before, Bosch and White [18] and Fornós et al. [37] proposed a classification for caves sediments in three groups depending on their origin: (1) slackwater sediments: allochthonous sediments associated to creep and saltation transport; (2) backswamp sediments: autochthonous sediments related to bedrock degradation processes followed by their accumulation inside the cave; and (3) reddish clay sediments: formed by suspended materials and classified as allochthonous. Based on the information and interpretations presented above, this classification has been applied to the sediments studied here.

Most of the samples in Area A correspond to allochthonous suspension materials that appear characterized by large material movement associated to saltation or creep processes. Only the inner sample (1AT and 2AT) are related to suspension processes (Table 6). One specific sample (4AT) has been interpreted as bioclastic gravels and sand of marine origin and could be associated with storm episodes [16].

Table 6. Summary table of all grain size samples analyzed. Relationship between sample type, grain size distribution, class and the principal deposition process (the sample may be affected by more overlapping processes) in relation with the presence or not of calcite. (* 4AT is the special sample formed by bioclasts).

Sample Type	Grain-Size Distribution	Class	Presence of Calcite	Principal Deposition Processes	
Area A					
1AT	Terrestrial	Bimodal	4	-	Suspension and Saltation or creep
2AT	Terrestrial	Bimodal	3	-	Saltation or creep and Suspension
3AT	Terrestrial	Unimodal	2	-	Saltation or creep
4AT	Terrestrial	Bimodal	3	Yes	* Saltation or creep
5AT	Terrestrial	Unimodal	2	-	Saltation or creep
6AS	Submerged	Unimodal	2	-	Saltation or creep
Area B					
1BT	Terrestrial	Bimodal	3	Yes	Bedrock degradation and Suspension
2BS	Submerged	Polymodal	5	Yes	Bedrock degradation
3BS	Submerged	Unimodal	1	-	Suspension
4BS	Submerged	Unimodal	1	Yes (little)	Suspension
5BS	Submerged	Unimodal	2	Yes	Bedrock degradation
6BS	Submerged	Bimodal	3	-	Saltation or creep and Suspension
Area C					
1CS	Submerged	Bimodal	3	Yes	Bedrock degradation and Suspension
2CS	Submerged	Bimodal	3	Yes	Bedrock degradation and Suspension
3CS	Submerged	Bimodal	3	Yes	Bedrock degradation and Suspension
4CS	Submerged	Unimodal	2	Yes (little)	Bedrock degradation
Area D					
1DT	Terrestrial	Bimodal	3	-	Saltation or creep and Suspension
2DT	Terrestrial	Unimodal	2	Yes (little)	Saltation or creep
3DT	Terrestrial	Unimodal	2	Yes	Bedrock degradation and Suspension
4DT	Terrestrial	Bimodal	3	Yes (little)	Saltation or creep and Suspension
5DT	Terrestrial	Polymodal	5	-	Saltation or creep and Suspension
6DT	Terrestrial	Bimodal	4	-	Suspension and Saltation or creep
7DT	Terrestrial	Bimodal	3	-	Saltation or creep and Suspension
8DT	Terrestrial	Bimodal	3	-	Saltation or creep and Suspension
Area E					
1ES	Submerged	Polymodal	5	-	Suspension
2ES	Submerged	Unimodal	1	-	Suspension
3ES	Submerged	Bimodal	4	Yes (little)	Suspension and Bedrock degradation
4ES	Submerged	Bimodal	4	Yes	Bedrock degradation and Suspension
5ES	Submerged	Polymodal	5	-	Suspension
6ES	Submerged	Polymodal	5	-	Suspension
	Soil	Unimodal	2	Yes (little)	Different process
	Soil	Unimodal	2	Yes (little)	Different process

The samples in area B that are located close to the terrestrial zone (D) present suspension materials, although some of them show a bedrock degradation population too. On the other part of the area, sample 5BS, which is the closest to the Ses Figueres cave entrance, is related to bedrock degradation, which is consistent with the formation of this entrance (associated with bedrock erosion and collapse). The other sample close to the Ses Figueres entrance (6BS) shows suspension and saltation or creep movement associated to material arrived from the outside (Table 6). Therefore, both allochthonous and autochthonous sediments are found in this sector of the cave.

Most of the samples from area C are formed by suspension materials and bedrock degradation (Table 6). Suspension populations of the sediments decrease towards the interior of the cave, while the populations associated to the rock degradation increase. The area D presents suspension, as well as saltation or creep materials, and bedrock degradation is almost absent (Table 6). The allochthonous suspension deposits seem to increase towards the interior of the cave.

Finally, in area E, most of the samples are composed by superposition of several suspension populations and bedrock degradation populations. The suspension populations decrease towards the interior of the cavity.

The soil samples are not included in this classification because they might have been affected by other types of sedimentary processes due to the fact that they are located outdoors.

The mineralogical trends observed in the samples clearly fit with what has been interpreted about the autochthonous or allochthonous origin of the sediments in each area of the cave (Table 6), linking the first group with submerged samples and the second with terrestrial ones.

As explained above, submerged samples are located on the floor inside the cave and are associated to autochthonous deposits that are mixed with some autochthonous materials whose mineralogical composition is related to carbonates (calcite and dolomite) and attributed to the bedrock erosion, weathering, and/or degradation. This process is the main factor of development in the coastal caves of Mallorca [24,25,27,37] and is directly associated to phreatic dissolution in the mixing zones and to the presence of the halocline [33]. In the sediments of the Ases cave, the highest contents of these minerals have been found in samples from the perpendicular to the general direction conduits and from the innermost zone of the cave (areas B, C, and E).

Terrestrial samples are located in filled wall and ceiling voids that may be associated to a previous cave filling stage followed by its subsequent washing. They are considered allochthonous deposits. These deposits do not contain large amounts of carbonates. Instead, detrital minerals, such as quartz, albite, or illitic phases, are more important, as also described in similar deposits from other caves in Mallorca [27].

Fornós et al. [30] assumed that all these sedimentary deposits located inside the Mallorca caves studied by them are allochthonous and associated to the deposition of the air suspended Sahara dust. The results found in this study demonstrate that the origin of these sediments cannot only be allochthonous but also autochthonous. Moreover, they indicate that the allochthonous deposits can be associated to the movement of material by different processes (suspension, saltation, or creep) related to water movements and not to air. Therefore, the possible presence of Sahara dust in these materials cannot be ruled out, but it is clear that not all the sedimentary deposits of the caves are formed of this dust.

The organic matter content analysis in the samples (Table 1) shows an average value lower than 5% and the difference between the content in the submerged samples (4.68%) and in the terrestrial ones (3.45%) is negligible to indicate any special pattern. This homogeneity in the organic matter content could be interpreted as associated to the development of the roots of the external plants directly (which in some areas can be seen on the ceiling of the cave) or by its transport through the infiltration [21,43].

The results obtained from the study of the samples color indicate a general reddish color with orange tones for all the samples without differentiation between sample type or

location. However, this color evidences the presence of clays and hematite, obtaining more reddish and less orange tones with greater amounts of this last mineral in the sample.

5.3. Clay Minerals Origin and Paleoenvironmental Interpretation

Clay minerals found in caves are frequently related to transported sediments and soils. Previous investigations reported detrital sediments containing kaolinite, smectite, and illite in other caves worldwide, e.g., [4,5,8,44]. In those cases, the clay minerals were formed during continental weathering processes and soil formation and then they were transported into the cave [13]. These clay minerals thus reflected the paleoenvironmental conditions of the region.

However, the clay minerals can also be inherited from the weathered bedrock or may even be formed inside the caves [4], in which case they reflect the paleoenvironmental conditions inside the cave.

The weathering processes transform part of the original silicates present in the sediment in clay minerals and the type of clay mineral dominant in the sediment is a good indicator of the kind and intensity of weathering responsible of its origin. Under dry and cold climates, where significant hydrolysis is absent, the production of clay minerals depends on the physical weathering, and the mineral assemblages are essentially dominated by illite [45–49]. By contrast, under warmer and more humid conditions, the effective hydrolysis caused by intense chemical weathering enhances the genesis of kaolinite and smectite [45]. This process has been described in other caves from Romania and Spain [11,20] where the authors described the in-situ transformation of the host rock into red clay-rich sediments formed by quartz, kaolinite, smectite, and montmorillonite (as well as iron oxides and hydroxides) by hydrolysis processes. In the sediments of the Ases Cave studied here, the presence of platy kaolinites with subhedral to euhedral morphologies (Figure 5) in the terrestrial and submerged sediments is not compatible with a detrital origin since the erosion and transport processes would have altered those morphologies [31,50,51]. An additional observation that supports this conclusion is the fact that the kaolinite crystals observed in the soil sample have anhedral morphologies (Figure 6f). Therefore, the kaolinite observed in the sediments of the cave may have an authigenic origin and not proceed from the surrounding soil.

As previously commented, the soil outside the cave has a poor development of the horizons and the operating processes (e.g., pedoturbation or bioturbation) may disturb the kaolinite morphology, causing its anhedral shape. In any case, the presence of this mineral is indicative of soil development outside the cave. Smectite was not found in the soil or in the bedrock samples, but it was detected in some of the submerged sediment samples. This indicates that smectite may also have formed in-situ. The flake-type morphologies observed in the smectite crystals are also compatible with an authigenic origin under weathering environments [52,53].

Illite in caves is usually considered a detrital mineral derived from the external soil or the bedrock [13]. As mentioned above, the genesis of the illitic phases is typical of physical weathering environments [31,54], and therefore its origin is not related to the origin of kaolinite. However, the presence of kaolinite crystals over the illitic phases plates (see Figure 6a) may indicate that the illitic phases form earlier and that they act as substrates for kaolinite crystallization, as described in other weathering environments involving soil development [51,55]. Smectite crystals have also been found over these illitic phases plates, indicating their genesis from the illite degradation [56–58]. Finally, the weathering of chlorite can also result in kaolinite [59], and thus the small quantities of chlorite detected in certain samples may also be, as in the case of the illitic phases, former phases.

In summary, kaolinite and smectite seem to have formed inside the cave as a consequence of the dissolution of previous aluminosilicates (e.g., feldspar, illitic phases, chlorite) during the chemical weathering of the allochthonous and autochthonous sediments of the cave [45,60].

The illitic phases and chlorite, on the other hand, seem to be former phases and with a probable detrital origin. The presence of authigenic kaolinite in the terrestrial and submerged sediments indicates an intense chemical weathering, which reflects a warm and humid environment in the cavities [50,60,61]. These conditions prevailed especially in those areas of the cave where the authigenic kaolinite content is higher (A and D area). On the other hand, although in lower content, kaolinite is in general more crystalline in the submerged samples, which could be related to rises of the water level that would keep the mineral submerged preventing its alteration after its genesis.

Water level fluctuations could also be responsible for smectite genesis. According to Polyak [19], the genesis of this mineral in caves takes place when the sediments are submerged by floodwater or saturated after the floodwater level descends. The presence of smectite in the submerged samples also indicates a less intense chemical weathering, which is also supported by the mineralogical tendency observed towards the interior of the cave with an increase in detrital quartz and illitic phase contents and a decrease in kaolinite, hematite, goethite, orthoclase, and albite contents.

6. Conclusions

The mineralogical and sedimentological study of the sediments located in the Ases cave allowed us to classify them and elucidate some differences in the sedimentary and environmental conditions of the different areas of the cave.

Terrestrial samples are mainly formed by quartz, albite, and clay minerals, which are related to allochthonous materials deposited in a previous stage of cave filling. The submerged samples are enriched in autochthonous calcite and dolomite inherited from the bedrock due to the dissolution in the mixing zones and to the presence of the halocline. These deposits are considered totally washed by the constant presence of water in those areas (as in the area D).

The study of the mineralogy and grain size of the deposits allows to differentiate the principal facies in each area of the cave: the area A is directly affected by the sea influence and present slackwater and reddish clay; the area B is affected by the presence of the Ses Figueres cave entrance, showing three different facies: slackwater, reddish clay, and backswamp; C and E areas are mainly formed by bedrock degradation and are composed by backswamp and reddish clays; and area D is mainly affected by its proximity to the main entrance, showing slackwater and reddish clay deposits.

Therefore, terrestrial samples are related to allochthonous origin and, in general, to slackwater and reddish silts and clay facies, while submerged samples are related to autochthonous origin and, in general, to backswamp facies. That is, the study shows that the sedimentary material inside the cave has different origins: autochthonous or allochthonous; and the allochthonous origin is not only related to the Sahara's dust.

The subhedral to euhedral kaolinite crystals in the cave sediments in comparison with the soil and the presence of smectite with flake morphologies only in the cave sediments suggest an authigenic origin for these minerals in the sediments of the cave and can thus, reflect variations in the weathering conditions inside the cave. Additionally, the growth of kaolinite on the illitic phases plates indicates that these illitic phases were formed earlier and are most probably detrital. The higher quantities of authigenic kaolinite in the terrestrial samples indicate intense chemical weathering conditions, affecting the detrital sediments and reflecting warm and humid environment conditions in the terrestrial areas of the cave. The decrease of kaolinite content together with the increase of detrital minerals (e.g., quartz and illitic phases) towards the interior of the cave indicates a decrease in the intensity of the chemical weathering. The presence of authigenic smectite in the submerged samples also indicates that decreases in the weathering intensity might especially have taken place in those areas where the water level increased.

In summary, three main conclusions can be highlighted: (1) The initial filling of the cave with allochthonous sediments occurred in the presence of water during humid periods. (2) The presence of terrestrial deposits in the emerged areas indicates that the water table

level (sea level) has probably not risen since their deposition. Otherwise, they would have been eroded. (3) The presence of high amounts of authigenic deposits in the submerged zones indicates the stability of the mixing zone, and consequently the sea level, over the time.

This work evidences the importance of the detailed study of these deposits to complement the understanding of the behavior of these complex karstic systems.

Supplementary Materials: The following supporting information can be downloaded at: <https://www.mdpi.com/article/10.3390/min12111473/s1>, Table S1: Relative proportions of the mineral phases detected in the whole rock and <2 µm fractions XRD patterns of the sediment samples in Dets Ases Cave; Table S2: Kaolinite crystallinity in the sediments from Dets Ases Cave measured in air-dried oriented aggregates; Table S3: Grain size analysis of Des Ases Cave; statistical results, classification and general composition.

Author Contributions: Conceptualization, E.L. and A.E.; methodology, E.L., A.E. and F.G.; formal analysis, E.L. and A.E.; investigation, E.L. and A.E.; resources, A.E. and F.G.; data curation, E.L. and A.E.; writing—original draft preparation, E.L. and A.E.; writing—review and editing, A.E., E.L., L.F.A. and J.J.F.; visualization, E.L. and A.E.; supervision, L.F.A. and J.J.F.; project administration, A.E. and E.L.; funding acquisition, J.J.F. All authors have read and agreed to the published version of the manuscript.

Funding: This research was funded by Agencia Estatal de Investigación (AEI), grant project number PID2020-112720GB-I00/AEI/10.13039/501100011033 and the Spanish Ministry of Science, Innovation and Universities with the grant received by A. Entrena (contract number BES-C2017-009) for development of her Ph.D.

Acknowledgments: The authors would also like to thank the Societat Espeleològica Balear (SEB) for the elaboration of the survey of the, and specifically to J.J. Ensenyat for his help throughout the field campaigns and with the cartography. Authors would like to acknowledge the use of Servicio General de Apoyo a la Investigación-SAI, Universidad de Zaragoza. The authors would also like to thank the comments and suggestions from M. Gimeno from the University of Zaragoza.

Conflicts of Interest: The authors declare no conflict of interest.

References

1. Cisneros, M.; Cacho, I.; Moreno, A.; Stoll, H.; Torner, J.; Català, A.; Edwards, R.L.; Cheng, H.; Fornós, J.J. Hydroclimate variability during the last 2700 years based on stalagmite multi-proxy records in the central-western Mediterranean. *Quat. Sci. Rev.* **2021**, *269*, 107–137. [[CrossRef](#)]
2. Moreno, A.; Pérez-Mejías, C.; Bartolomé, M.; Sancho, C.; Cacho, I.; Stoll, H.; Delgado-Huertas, A.; Hellstrom, J.; Edwards, R.L.; Cheng, H. New speleothem data from Molinos and Ejulve caves reveal Holocene hydrological variability in northeast Iberia. *Quat. Res.* **2017**, *88*, 223–233. [[CrossRef](#)]
3. Bernal-Wormull, J.L.; Moreno, A.; Pérez-Mejías, C.; Bartolomé, M.; Aranburu, A.; Arriolabengoa, M.; Iriarte, E.; Cacho, I.; Spötl, C.; Edwards, E.L.; et al. Immediate temperature response in northern Iberia to last deglacial changes in the North Atlantic. *Geology* **2021**, *49*, 999–1003. [[CrossRef](#)]
4. Polyak, V.J.; Güven, N. Clays in caves of the Guadalupe Mountains, New Mexico. *J. Caves Karst Stud.* **2000**, *62*, 120–126.
5. Albani, A.E.; Meunier, A.; Macchiarelli, R.; Ploquin, F.; Tournepiche, J.F. Local environmental changes recorded by clay minerals in a karst deposit during MIS 3 (La Chauverie, SW France). *Quat. Int.* **2011**, *241*, 26–34. [[CrossRef](#)]
6. van Hengstum, P.J.; Scott, D.B.; Gröcke, D.R.; Charette, M.A. Sea level controls sedimentation and environments in coastal caves and sinkholes. *Mar. Geol.* **2011**, *286*, 35–50. [[CrossRef](#)]
7. Ford, D.; Williams, P.D. *Karst Hydrogeology and Geomorphology*; 1st Chichester; John Wiley & Sons: Hoboken, NJ, USA, 2007; p. 562.
8. Foss, A.M.; Sasowsky, I.D.; Larock, E.J.; Kambesis, P.N. Detrital origin of a sedimentary fill, Lechuguilla Cave, Guadalupe Mountains, New Mexico. *Clays Clay Miner.* **2000**, *48*, 693–698. [[CrossRef](#)]
9. Osborne, R.A.L.; Zwingmann, H.; Pogson, R.E.; Colchester, D. Carboniferous clay deposits from Jenolan Caves, New South Wales: Implications for timing of speleogenesis and regional geology. *Aust. J. Earth Sci.* **2006**, *53*, 377–405. [[CrossRef](#)]
10. Iriarte, E.; Foyo, A.; Sánchez, M.A.; Tomillo, C.; Setién, J. The origin and geochemical characterization of red ochres from the Tito Bustillo and Monte Castillo caves (Northern Spain). *Archaeometry* **2009**, *51*, 231–251. [[CrossRef](#)]
11. Martín-García, R.; Martín-Pérez, A.; Alonso-Zarza, A.M. Weathering of host rock and corrosion over speleothems in Castañar cave, Spain: An example of a complex meteoric environment. *Carbonates Evaporites* **2011**, *26*, 83–94. [[CrossRef](#)]
12. Robert, C.; Chamley, H. Late Eocene-Early Oligocene Evolution of Climate and Marine Circulation: Deep-Sea Clay Mineral Evidence. *Antarct. Paleoenviro.* **1992**, *56*, 97–118.

13. Huang, S.; Hong, H.; Liao, W.; Wang, C.; Cheng, L.; Hao, X.; Li, D.; Bae, C.J.; Wang, W. Late Pleistocene paleoenvironment of southern China: Clay mineralogical and geochemical analyses from Luna Cave, Guangxi, China. *Quat. Int.* **2020**, *563*, 78–86. [[CrossRef](#)]
14. Onac, B.P.; Hutchinson, S.M.; Geantă, A.; Forray, F.L.; Wynn, J.G.; Giurgiu, A.M.; Coroiu, I. A 2500-year late Holocene multi-proxy record of vegetation and hydrologic changes from a cave guano-clay sequence in SW Romania. *Quat. Res.* **2015**, *83*, 437–448. [[CrossRef](#)]
15. Iacoviello, F.; Martini, I. Clay minerals in cave sediments and terra rossa soils in the Montagnola Senese karst massif (Italy). *Geol. Q.* **2013**, *57*, 527–536. [[CrossRef](#)]
16. Fornós, J.J.; Ginés, J.; Gràcia, F.; Merino, A. Els sediments de les cavitats càrstiques de les Balears. *Monogr. Soc. Hist. Nat. Balear.* **2011**, *17*, 199–212.
17. Zaharia, L.; Tămaş, T.; Suciuc-Krausz, E. Mineralogy of Cave No. 4 from Runcului Hill (Metaliferi Mts., Romania). *Theor. Appl. Karstol.* **2003**, *16*, 41–46.
18. Bosch, R.F.; White, W.B. Lithofacies and transport of clastic sediments in karstic aquifers. In *Stud. Cave Sediments*, 1st ed.; Sasowsky, I.D., Mylroie, J., Eds.; Springer: Boston, MA, USA, 2004; pp. 11–22. [[CrossRef](#)]
19. Polyak, V.J. Clays and Associated Minerals in Caves of the Guadalupe Mountains, New Mexico. Ph.D. Thesis, Texas Tech University, Lubbock, TX, USA, 1998.
20. Tămaş, T.; Kristály, F.; Barbu-Tudoran, L. Mineralogy of Iza Cave (Rodnei Mountains, N. Romania). *Int. J. Speleol.* **2011**, *40*, 171–179. [[CrossRef](#)]
21. Ginés, J.; Ginés, A.; Gràcia, F.; Fornós, J.J. L'espeleogènesi de les Coves del Drac (Manacor, Mallorca): Evolució dels coneixements i interpretació actual. *Pap. Soc. Espeleo. Balear* **2018**, *1*, 141–163.
22. Ginés, J.; Ginés, A. Las Coves del Drac (Manacor, Mallorca). *Endins Publ. D'espeleol.* **1992**, *17–18*, 5–20.
23. Gràcia, F.; Jaume, D.; Ramis, J.; Fornós, J.J.; Bover, P.; Clamor, B.; Gual, M.À.; Vadell, M. Les coves de Cala Anguila (Manacor, Mallorca). II: La Cova genovesa o cova d'en Bessó. Espeleogènesi, geomorfologia, hidrologia, sedimentologia, fauna, paleontologia, arqueologia i conservació. *Endins* **2003**, *25*, 43–86.
24. Gràcia, F.; Clamor, B.; Jaume, D.; Fornós, J.J.; Uriz, M.J.; Martin, D.; Gil, J.; Gràcia, P.; Febrer, M.; Pons, G. La Cova des Coll (Felanitx, Mallorca): Espeleogènesi, geomorfologia, hidrologia, sedimentologia, fauna i conservació. *Endins* **2005**, *27*, 141–186.
25. Gràcia, F.; Clamor, B.; Fornós, J.J.; Jaume, D.; Febrer, M. El sistema Pirate-Pont-Piqueta (Manacor, Mallorca): Geomorfologia, espeleogènesi, hidrologia, sedimentologia i fauna. *Endins* **2006**, *28*, 25–64.
26. Fornós, J.; Gràcia, F. Datació dels sediments recents que rebleixen les cavitats de Sa Gleda i del Sistema Pirata—Pont—Piqueta: Primeres dades. *Endins* **2007**, *31*, 97–100.
27. Gràcia, F.; Fornós, J.J.; Clamor, B.; Febrer, M.; Gamundí, P.; La Cova de Sa Gleda, I. Sector Clàssic, Sector de Ponent i Sector Cinc-Cents (Manacor, Mallorca): Geomorfologia, espeleogènesi, sedimentologia i hidrologia. *Endins* **2007**, *31*, 43–96.
28. Fornós, J.J.; Ginés, J.; Merino, A.; Bover, P. El rebliment sedimentari de la galeria del Tragus a la cova des Pas de Vallgornera (Llucmajor, Mallorca). *Bolleti Soc. D'hist. Nat. Balear.* **2010**, *53*, 179–191.
29. Ginés, À.; Ginés, J. Características espeleològiques del karst de Mallorca. *Endins* **1987**, *13*, 3–19.
30. Fornós, J.J.; Crespi, D.; Fiol, L.A. Aspectes mineralògics i texturals de la pols procedent de les pluges de lang a les Illes Balears: La seva importància en alguns processos geològics recents. *Bolleti Soc. D'hist. Nat. Balear.* **1997**, *40*, 113–122.
31. Laita, E.; Bauluz, B.; Aurell, M.; Bádenas, B.; Canudo, J.I.; Yuste, A. A change from warm/humid to cold/dry climate conditions recorded in lower Barremian clay-dominated continental successions from the SE Iberian Chain (NE Spain). *Sediment. Geol.* **2020**, *403*, 105673. [[CrossRef](#)]
32. Gràcia, F.; Watkinson, P.; Monserrat, T.; Landreth, R.; Clarke, O. Les coves de la zona de ses Partions—PortoColom (Felanitx, Mallorca). *Endins* **1997**, *21*, 5–36.
33. Tuccimei, P.; Soligo, M.; Ginés, J.; Ginés, A.; Fornós, J.J.; Kramers, J.; Villa, I.M. Constraining Holocene Sea levels using U-Th ages of phreatic overgrowths on speleothems from coastal caves in Mallorca (Western Mediterranean). *Earth Surf. Process. Landf.* **2010**, *35*, 782–790. [[CrossRef](#)]
34. Ginés, J.; Ginés, A.; Fornós, J.J. Dades sobre paleocarst i espeleocronologia de les Illes Balears. *Monogr. Soc. D'hist. Nat. Balear.* **2011**, *17*, 213–226.
35. Ginés, J.; Ginés, À. Les coves turístiques de les Illes Balears: Antecedents i estat de la qüestió. *Endins Publ. D'espeleol.* **2011**, *17*, 333–344.
36. Jaume, D.; Gràcia, F. Coves amb hàbitats anquihalins de les Balears i coves amb hàbitats dolçaquícules no litorals: Catàleg espeleològic i faunístic. *Endins* **2006**, *30*, 71–82.
37. Fornós, J.J.; Ginés, J.; Gràcia, F. Present-day sedimentary facies in the coastal karst caves of Mallorca Island (Western Mediterranean). *J. Cave Karst Stud.* **2009**, *71*, 86–99.
38. Gràcia, F.; Clamor, B.; Gamundí, P.; Fornós, J.J.; Watkinson, P. Cavitats subaquàtiques de la franja litoral de Mallorca. *Monogr. Soc. D'hist. Nat. Balear.* **2011**, *17*, 103–132.
39. Folk, R.L.; Ward, W.C. Brazos river bar: A Study in the Significance of Grain-Size Parameters. *J. Sediment. Res.* **1957**, *27*, 3–26. [[CrossRef](#)]
40. Blott, S.J.; Pye, K. GRADISTAT: A grain size distribution and statistics package for the analysis of unconsolidated sediments. *Earth Surf. Process. Landf.* **2001**, *26*, 1237–1248. [[CrossRef](#)]

41. Biscaye, P.E. Mineralogy and sedimentation of recent deep-sea clay in the Atlantic Ocean and adjacent seas and oceans. *Geol. Soc. Am. Bull.* **1965**, *76*, 803–832. [[CrossRef](#)]
42. Visher, G.S. Grain size distributions and depositional processes. *J. Sediment. Res.* **1969**, *39*, 1074–1106.
43. Beddows, P.A.; Mandić, M.; Ford, D.C.; Schwarcz, H.P. Oxygen and hydrogen isotopic variations between adjacent drips in three caves at increasing elevation in a temperate coastal rainforest, Vancouver Island, Canada. *Geochim. Cosmochim. Acta* **2016**, *172*, 370–386. [[CrossRef](#)]
44. Iacovello, F.; Martini, I. Provenance and geological significance of red mud and other clastic sediments of the Mugnano Cave (Montagnola Senese, Italy). *Int. J. Speleol.* **2012**, *41*, 317–328. [[CrossRef](#)]
45. Velde, B. *Origin and Mineralogy of Clays: Clays and the Environment*, 1st ed.; Springer: Berlin/Heidelberg, Germany; New York, NY, USA, 1995; p. 334.
46. Dhillon, S.K. Characterisation of potassium in Red (Alfisols), Black (Vertisols) and Alluvial (Inceptisols and Entisols) soils of India using electro-ultrafiltration. *Geoderma* **1991**, *50*, 185–196. [[CrossRef](#)]
47. Do Campo, M.; Bauluz, B.; del Papa, C.; White, T.; Yuste, A.; Mayayo, M.J. Evidence of cyclic climatic changes recorded in clay mineral assemblages from a continental Paleocene-Eocene sequence, northwestern Argentina. *Sediment. Geol.* **2018**, *368*, 44–57. [[CrossRef](#)]
48. Liu, Y.; Song, C.; Meng, Q.; He, P.; Yang, R.; Huang, R.; Chen, S.; Wang, D.; Xing, Z. Paleoclimate change since the Miocene inferred from clay-mineral records of the Jiuquan Basin, NW China. *Palaeogeogr. Palaeoclimatol. Palaeoecol.* **2020**, *550*, 109730. [[CrossRef](#)]
49. Deconinck, J.F.; Hesselbo, S.P.; Debuisser, N.; Averbuch, O.; Baudin, F.; Bessa, J. Environmental controls on clay mineralogy of an early jurassic mudrock (blue lias formation, southern England). *Int. J. Earth Sci.* **2003**, *92*, 255–266. [[CrossRef](#)]
50. Bauluz, B.; Yuste, A.; Mayayo, M.J.; Canudo, J.I. Early kaolinization of detrital Weald facies in the Galve Sub-basin (Central Iberian Chain, north-east Spain) and its relationship to palaeoclimate. *Cretac. Res.* **2014**, *50*, 214–227. [[CrossRef](#)]
51. Laita, E.; Bauluz, B.; Aurell, M.; Bádenas, B.; Yuste, A. Weathering events recorded in uppermost Hauterivian–lower Barremian clay-dominated continental successions from the NW Iberian Range: Climatic vs. tectonic controls. *J. Iber. Geol.* **2021**, *48*, 45–63. [[CrossRef](#)]
52. Buatier, M.D.; Karpoff, A.M.; Charpentier, D. Clays and zeolite authigenesis in sediments from the flank of the Juan de Fuca Ridge. *Clay Miner.* **2002**, *37*, 143–155. [[CrossRef](#)]
53. Ehrmann, W.; Setti, M.; Marinoni, L. Clay minerals in Cenozoic sediments off Cape Roberts (McMurdo Sound, Antarctica) reveal palaeoclimatic history. *Palaeogeogr. Palaeoclimatol. Palaeoecol.* **2005**, *229*, 187–211. [[CrossRef](#)]
54. Bauluz, B.; Mayayo, M.J.; Fernandez-Nieto, C.; Lopez, J.M.G. Geochemistry of Precambrian and Paleozoic siliciclastic rocks from the Iberian Range (NE Spain): Implications for source-area weathering, sorting, provenance, and tectonic setting. *Chem. Geol.* **2000**, *168*, 135–150. [[CrossRef](#)]
55. Bauluz, B.; Mayayo, M.J.; Yuste, A.; González López, J.M. Genesis of kaolinite from Albian sedimentary deposits of the Iberian Range (NE Spain): Analysis by XRD, SEM and TEM. *Clay Miner.* **2008**, *43*, 459–475. [[CrossRef](#)]
56. Jeong, G.Y.; Hillier, S.; Kemp, R.A. Changes in mineralogy of loess–paleosol sections across the Chinese Loess Plateau. *Quat. Res.* **2011**, *75*, 245–255. [[CrossRef](#)]
57. Schaetzl, R.; Thompson, M.L. *Soils: Genesis and Geomorphology*, 2nd ed.; Cambridge University Press: Cambridge, UK, 2015; p. 779.
58. Shrivastava, J.P.; Chandra, R. Pedogenically degenerated illite and chlorite lattices aid to palaeoclimatic reconstruction for chronologically constrained (8–130 ka) loess-palaeosols of Dilpur Formation, Kashmir, India. *Geosci. Front.* **2020**, *11*, 1353–1367.
59. Murakami, T.; Isobe, H.; Sato, T.; Ohnuki, T. Weathering of chlorite in a quartz-chlorite schist: I. Mineralogical and chemical changes. *Clays Clay Miner.* **1996**, *44*, 244–256. [[CrossRef](#)]
60. Chamley, H. Clay formation through weathering. In *Clay Sedimentology*, 1st ed.; Springer: Berlin/Heidelberg, Germany, 1989; pp. 21–50.
61. Raucskik, B.; Varga, A. Climato-environmental controls on clay mineralogy of the Hettangian-Bajocian successions of the Mecsek Mountains, Hungary: An evidence for extreme continental weathering during the early Toarcian oceanic anoxic event. *Palaeogeogr. Palaeoclimatol. Palaeoecol.* **2008**, *265*, 1–13. [[CrossRef](#)]